



Published in final edited form as:

Nature. 2013 January 24; 493(7433): 532–536. doi:10.1038/nature11713.

## Rapid regulation of depression-related behaviors by control of midbrain dopamine neurons

Dipesh Chaudhury<sup>1,\*</sup>, Jessica J. Walsh<sup>1,2,\*</sup>, Allyson K. Friedman<sup>1</sup>, Barbara Juarez<sup>1,2</sup>, Stacy M. Ku<sup>1,2</sup>, Ja Wook Koo<sup>2</sup>, Deveroux Ferguson<sup>2</sup>, Hsing-Chen Tsai<sup>3</sup>, Lisa Pomeranz<sup>4</sup>, Daniel J. Christoffel<sup>2</sup>, Alexander R. Nectow<sup>4</sup>, Mats Ekstrand<sup>4</sup>, Ana Domingos<sup>4</sup>, Michelle Mazie-Robison<sup>2</sup>, Ezekiel Mouzon<sup>2</sup>, Mary Kay Lobo<sup>2</sup>, Rachael L. Neve<sup>5</sup>, Jeffrey M. Friedman<sup>4</sup>, Scott J. Russo<sup>2</sup>, Karl Deisseroth<sup>3</sup>, Eric J. Nestler<sup>1,2</sup>, and Ming-Hu Han<sup>1,2,†</sup>

<sup>1</sup>Department of Pharmacology and Systems Therapeutics, Friedman Brain Institute, Mount Sinai School of Medicine, New York, NY 10029, USA

<sup>2</sup>Fishberg Department of Neuroscience, Friedman Brain Institute, Mount Sinai School of Medicine, New York, NY 10029, USA

<sup>3</sup>Departments of Bioengineering and Psychiatry and Behavioural Sciences, Stanford University, Stanford, CA 94305, USA

<sup>4</sup>Laboratory of Molecular Genetics, Rockefeller University, New York, NY 10056, USA

<sup>5</sup>McGovern Institute for Brain Research, Massachusetts Institute of Technology, Cambridge, MA 02139, USA

### Abstract

Ventral tegmental area (VTA) dopamine (DA) neurons in the brain's reward circuit play a crucial role in mediating stress responses<sup>1–4</sup> including determining susceptibility *vs.* resilience to social stress-induced behavioural abnormalities<sup>5</sup>. VTA DA neurons exhibit two *in vivo* patterns of firing: low frequency tonic firing and high frequency phasic firing<sup>6–8</sup>. Phasic firing of the neurons, which is well known to encode reward signals<sup>6,7,9</sup>, is upregulated by repeated social defeat stress, a highly validated mouse model of depression<sup>5,8,10–13</sup>. Surprisingly, this pathophysiological effect is seen in susceptible mice only, with no change in firing rate apparent in resilient individuals<sup>5,8</sup>. However, direct evidence linking—in real-time—DA neuron phasic firing in promoting the susceptible (depression-like) phenotype is lacking. Here, we took advantage of the temporal precision and cell type- and projection pathway-specificity of optogenetics to demonstrate that enhanced phasic firing of these neurons mediates susceptibility to social defeat stress in freely behaving mice. We show that optogenetic induction of phasic, but not tonic, firing, in VTA DA

Users may view, print, copy, download and text and data- mine the content in such documents, for the purposes of academic research, subject always to the full Conditions of use: [http://www.nature.com/authors/editorial\\_policies/license.html#terms](http://www.nature.com/authors/editorial_policies/license.html#terms)

<sup>†</sup>Corresponding author: M.H.H. ([ming-hu.han@mssm.edu](mailto:ming-hu.han@mssm.edu)).

\*These authors contributed equally

**Author information.** Mary Kay Lobo's present address is Department of Anatomy and Neurobiology, University of Maryland School of Medicine, 20 Penn Street Rm S251, Baltimore, MD 21201.

**Author contribution.** D.C., J.J.W., A.K.F., B.J., J.W.K., D.F., D.J.C., H.C.T., M.K.L., M.M.R., and S.K. collected and analyzed data. L.P., A.R.N. Z.M., M.E., R.L.N., E.M., S.J.R., J.M.F., K.D. and E.J.N. generated and provided viral vectors and TH-Cre mice. D.C., J.J.W., E.J.N. and M.H.H. designed and wrote the paper.

neurons of mice undergoing a subthreshold social defeat paradigm rapidly induced a susceptible phenotype as measured by social avoidance and decreased sucrose preference. Optogenetic phasic stimulation of these neurons also quickly induced a susceptible phenotype in previously resilient mice that had been subjected to repeated social defeat stress. Furthermore, we show differences in projection pathway-specificity in promoting stress susceptibility: phasic activation of VTA neurons projecting to the nucleus accumbens (NAc), but not to the medial prefrontal cortex (mPFC), induced susceptibility to social defeat stress. Conversely, optogenetic inhibition of the VTA-NAc projection induced resilience, while inhibition of the VTA-mPFC projection promoted susceptibility. Overall, these studies reveal novel firing pattern- and neural circuit-specific mechanisms of depression.

---

To selectively target VTA DA neurons, we injected a Cre-dependent adeno-associated virus (AAV) vector expressing channelrhodopsin-2 (ChR2)-EYFP (AAV-DIO-ChR2-EYFP) into the VTA of tyrosine hydroxylase (TH)-Cre transgenic mice<sup>7,14</sup>. We first validated the specificity and efficacy of AAV-DIO-ChR2-EYFP expression in VTA DA neurons of TH-Cre mice *in vivo* (Fig. 1a–b). Next, functional validation of ChR2-EYFP expression in VTA DA neurons using *in vitro* and *in vivo* electrophysiological recordings confirmed that optogenetic stimulation enables precise temporal control of these neurons (Supplementary Fig. 1a–c) and can be used to mimic the *in vivo* pathophysiological upregulation in phasic firing seen in the social defeat stress model of depression<sup>8,12</sup>.

To investigate the functional significance of the increase in phasic firing of VTA DA neurons observed after repeated (10-day) social defeat stress, we examined the effect of optogenetically inducing tonic (0.5 Hz) or phasic (20 Hz) firing (Fig. 1c; 5 spikes for each 10 seconds) in ChR2-expressing VTA DA neurons of TH-Cre mice while undergoing subthreshold exposure to social defeat (Fig. 1d). Mice that undergo this subthreshold paradigm do not exhibit social avoidance or other depression-like behaviours (Supplementary Fig. 1d), but they are more vulnerable to subsequent stress<sup>5,15</sup>. We stimulated VTA DA neurons during the subthreshold defeat paradigm and measured social interaction and sucrose preference as two sequelae of defeat stress: social avoidance and reduced sucrose preference characterize the susceptible phenotype induced by our repeated (10-day) social defeat paradigm<sup>5,8,10</sup>. Mice that received phasic stimulation exhibited a robust increase in the depression-like phenotype as indicated by the significant decrease both in social interaction in the presence of a target mouse (Fig. 1e and Supplementary Fig. 1e–g) and in sucrose preference (Fig. 1f) compared to both tonic stimulated ChR2-EYFP mice and phasic stimulated EYFP control mice. These data confirm the functional importance of increased phasic, but not tonic, firing of VTA DA neurons during exposure to stress for promoting susceptibility for depression-like behavioural abnormalities.

To directly test the causal link between phasic DA neuron firing and stress susceptibility, mice were exposed to subthreshold defeat followed by stimulation of VTA DA neurons *during* the social interaction test (Supplementary Fig. 2a). Phasic stimulation of VTA DA neurons instantly induced a susceptible phenotype (increased social avoidance) during the social interaction test in the presence of a target CD1 mouse (or a target C57 mouse, Supplementary Fig. 3), an effect not seen in tonic stimulated ChR2 mice or phasic

stimulated EYFP control mice (Fig. 2a and Supplementary Fig. 2b–d). ChR2-expressing mice that received phasic stimulation during the brief 2.5 min social interaction test also exhibited reduced sucrose preference compared to tonic stimulated ChR2 mice or phasic stimulated EYFP control mice (Fig. 2b). These findings are striking because they reveal the rapid induction of such depression-like behaviours that normally require repeated social defeat stress.

In contrast to the ability of VTA DA neuron stimulation in promoting depression-like behaviours either during or after social defeat stress, we found that phasic stimulation of these neurons in naive animals had no effect on social interaction, on sucrose preference, or on baseline anxiety-related measures (Supplementary Fig. 4). These findings demonstrate that the pro-depression-like effects of VTA DA neuron activation demonstrated here are context-specific, an important finding in light of the pro-reward consequences of such DA neuron activation in other systems<sup>6,7,9</sup>. Furthermore, chronic mild stressors, or physically aversive stimuli, inhibit the activity of VTA DA neurons, while more severe stressors increase activity<sup>16,17</sup>, as we see with severe social stress. Also, chronic mild stress and chronic social defeat stress have been shown recently to produce different changes in extracellular levels of several neurotransmitters in a number of brain areas<sup>18</sup>. These findings raise the possibility that, in addition to context, the severity of stress is another important determinant of stress regulation of DA neuron firing.

We next investigated whether phasic firing of VTA DA neurons could convert resilient mice to susceptible mice. Utilizing our standard repeated (10-day) social defeat paradigm<sup>5,8,10</sup>, we identified the subgroup of mice that remained resilient based on normal social interaction scores, which we know are highly correlated with normal sucrose preference and other behavioural and biochemical endpoints<sup>5</sup>. Our previous work had demonstrated that VTA DA neurons of resilient mice display normal firing rates and patterns due to unique adaptations within these neurons that prevent the stress-induced increase in their excitability<sup>5,8</sup>. To test the effect of increased phasic stimulation of VTA DA neurons in resilient mice, we switched to herpes simplex virus (HSV)-ChR2 and control vectors with confirmed immunohistochemical and functional validation (Supplementary Fig. 5a–d).

HSV vectors have the advantage of expressing their transgenes very rapidly (within 24 hr) as opposed to AAV vectors, which require 10–14 days for maximal expression<sup>5,10,14</sup>. In this experiment, wild type mice were put through the standard repeated social defeat stress followed by a social interaction test on day 11 to identify the resilient mice as noted above. Resilient mice were injected with HSV-EYFP or HSV-ChR2-EYFP and subsequently analyzed in a second social interaction test during which time they underwent optogenetic phasic stimulation (Supplementary Fig. 5e–f). While optogenetically stimulated HSV-EYFP-injected mice remained resilient, optically induced phasic firing of the VTA of HSV-ChR2-EYFP injected mice instantly converted their behavioural phenotype from resilient to susceptible as evidenced by the decrease in time spent in the interaction zone (Fig. 2c and Supplementary Fig. 5g–i). Furthermore, such phasic firing of the VTA induced anhedonic traits as evidenced by decreased sucrose preference compared to HSV-EYFP-injected mice (Fig. 2d).

Given the striking impairment in sucrose preference ~12 hr after the optogenetic activation of VTA neurons, we hypothesized that such stimulation might induce lasting changes in VTA DA neuron excitability. To investigate this hypothesis, we measured intrinsic membrane properties of these neurons of TH-Cre mice that had previously undergone the subthreshold social defeat paradigm followed by *in vivo* opto-stimulation during the social interaction test (Supplementary Fig. 5j). Phasic stimulation induced increased VTA DA neuronal excitability compared to EYFP and tonic stimulated mice as measured by increased spontaneous (Fig. 2e) and evoked (Fig. 2f–g) activity 8–12 hr after optical stimulation. These findings suggest that subthreshold defeat followed by acute optogenetic activation leads to long-lasting neuroadaptations in VTA DA neurons that underlie the sustained decrease in sucrose preference observed.

VTA DA neurons project broadly throughout the brain. The VTA-NAc pathway is well established for its role in reward<sup>6,9,14</sup>, but has also been implicated in stress responses, as has the VTA-mPFC pathway<sup>1,2,4,5,10,19</sup>. Therefore, we were interested in investigating the role of these two distinct VTA projection pathways in promoting the susceptible and resilient phenotypes. We first investigated the VTA-NAc circuit by specifically labeling VTA neurons projecting to the NAc; this was accomplished by injecting the retrograde green fluorescent tracer lumafluor into the NAc and measuring the firing rate of dye-positive VTA-NAc neurons in control, susceptible, and resilient mice after repeated (10-day) social defeat stress (see Supplementary Fig. 6a–b for anatomical validation). We found, in brain slices, that NAc-projecting VTA DA neurons of susceptible mice exhibited a significantly higher firing rate compared to those of control and resilient mice (Fig. 3a–b), which is in agreement with increased phasic firing events from our previous work<sup>5,8</sup>. Next, we used optogenetic techniques to selectively stimulate this VTA-NAc pathway. To do this, we injected the retrograde travelling pseudorabies virus expressing Cre (PRV-Cre) into the NAc and the Cre-dependent AAV-DIO-ChR2-EYFP into the VTA of wild type mice (Supplementary Fig. 6c). Immunohistochemical and electrophysiological validation confirmed the viability of using PRV-Cre to express functional ChR2 in VTA cells projecting to NAc (Supplementary Fig. 6d–h). Mice were then subjected to the subthreshold social defeat paradigm and 24 hr later were optogenetically stimulated during the social interaction test (Supplementary 6i). Optical induction of phasic, but not tonic, firing in VTA-NAc neurons induced the susceptible phenotype as measured by increased social avoidance and decreased sucrose preference (Fig. 3c–d and Supplementary 6j–k). While the vast majority of DA neurons in this pathway were optically stimulated, only a small number of non-DA neurons were labeled with our approaches. Further work will be needed to study any potential influence of these non-DA cells on stress responses.

To investigate the effect of inhibiting the VTA-NAc pathway on the expression of the stress response, we injected AAV-DIO-halorhodopsin (NpHR)-EYFP (version 3.0) into the VTA followed by PRV-Cre in the NAc (Supplementary Fig. 7a–b). Functional validation confirmed that yellow light (563 nm) reliably inhibited VTA neuronal firing both *in vitro* and *in vivo* (Supplementary Fig. 7c–d), and importantly, with the light protocol we used during the behavioural experiments, we did not observe any NpHR-activated rebound effect in these neurons (Supplementary Fig. 7e). Furthermore, anatomical quantification showed

robust NpHR expression in VTA cells projecting to NAc (Supplementary Fig. 7f–g). Mice were first put through the standard repeated social defeat stress paradigm followed by a social interaction test on day 11 to identify the susceptible mice for EYFP control and NpHR groups (Supplementary Fig. 7h). Optogenetically stimulated DIO-EYFP injected mice remained susceptible in the second social interaction test (both during target presence and absence) while inhibition of the VTA-NAc projection of DIO-NpHR-EYFP injected mice instantly induced the resilient phenotype as evidenced by the increase in both the amount of time spent in the interaction zone and preference for sucrose (Fig. 3e–f and Supplementary Fig. 7i–j). These mice had undergone a chronic social defeat paradigm and an earlier social interaction test. It is therefore likely that the optogenetic attenuation of the increased activity of the VTA-NAc pathway, that is typically seen in susceptible mice, combined with reactivation of the memory of the previous social interaction test, resulted in those NpHR-injected mice spending longer times in the interaction zone, both in the absence and presence of a target mouse, during the second social interaction test.

We also carried out experiments to investigate the functional importance of mPFC-projecting VTA DA neurons in promoting a susceptible phenotype (Fig. 4). We first labeled VTA neurons projecting to mPFC by injecting the retrograde red fluorescent tracer lumafloour into the mPFC (Supplementary Fig. 8a–b). Surprisingly, the firing rate of VTA-mPFC neurons was dramatically decreased in brain slices obtained from susceptible mice after repeated (10-day) social defeat stress, as compared to that of control and resilient mice (Fig. 4a–b). This is consistent with a recent report of decreased extracellular dopamine levels in this region after repeated social defeat stress<sup>18</sup>. Next, we used optogenetic techniques to selectively stimulate the VTA-mPFC pathway. To do this, we injected the retrograde PRV-Cre viral vector into the mPFC and the Cre-dependent AAV-DIO-ChR2-EYFP into the VTA of wild type mice (Supplementary Fig. 8c), and confirmed the viability of using PRV-Cre to express functional ChR2 in VTA cells projecting to mPFC (Supplementary Fig. 8d–h). Optically-induced phasic firing of these VTA-mPFC neurons, during the social interaction test in mice that had previously undergone subthreshold social defeat, had no effect on social interaction and sucrose preference as compared to tonic stimulation and control viral vectors (Fig. 4c–d and Supplementary Fig. 8i–j). We next investigated the effect of inhibiting the VTA-mPFC pathway on the expression of the stress response by injecting DIO-NpHR-EYFP into the VTA followed by PRV-Cre into the mPFC (Supplementary Fig. 9a–d). *In vivo* optical inhibition of the VTA-mPFC pathway by activation of NpHR, during the social interaction test in mice that had previously undergone subthreshold social defeat, induced the susceptible phenotype compared to control mice as measured by decreased social interaction (Fig. 4e and Supplementary Fig. 9e–f). Interestingly, there was no difference in sucrose preference (Fig. 4f).

Our study establishes a direct link between VTA DA neuronal firing patterns and susceptibility to a depression-related phenotype, where phasic firing of NAc-projecting VTA DA neurons encodes a signal for susceptibility. This finding is consistent with the hypothesized role of VTA-NAc (mesolimbic) DA neuronal phasic firing in this stress model: we previously showed that the VTA-NAc pathway is a key determinant of susceptibility *vs.* resilience to repeated social defeat stress<sup>5</sup>, and that the pathophysiological

increase in phasic firing occurs selectively in susceptible mice<sup>8</sup>. The observation that VTA DA neuron phasic firing has a functional role in encoding for both depression-like symptoms following social defeat stress, and conditioned place preference<sup>7</sup>, suggests that firing patterns of these neurons and the subsequent encoding of the depressive or reward phenotype are highly context-dependent. Such encoding of stress versus reward is more complex still, because it is not only firing pattern selective<sup>7</sup>, but also is dependent on the severity of stress (as noted above) and exhibits clear projection pathway specificity<sup>19</sup>.

Additionally, our observation of the rapid onset of the susceptible phenotype in response to optical stimulation corresponds to the implicated function of mesolimbic DA neurons in mediating rapid antidepressant effects<sup>1,20</sup>. Similarly, hyperpolarization-activated cation channels ( $I_h$ ), a key channel responsible for the transition from tonic to phasic firing of VTA DA neurons<sup>21,22</sup> that is highly expressed in VTA-NAc neurons<sup>19</sup>, is increased in susceptible mice, while, conversely,  $I_h$  inhibitors display rapid and long-lasting antidepressant efficacy<sup>8,23</sup>. The rapid antidepressant effects of ketamine<sup>24–26</sup>, sleep deprivation<sup>27</sup>, and deep brain stimulation<sup>28–30</sup> further support the existence of rapidly reversible brain mechanisms and circuit regulation for depression treatment. Consistent with these studies, we show a rapid ‘rescue’ effect of VTA-NAc pathway inhibition when it occurs in the context of repeated severe social stress. In striking contrast, our findings that the VTA-mPFC pathway serves an opposite function, as compared to the VTA-NAc pathway, are consistent with a recent study demonstrating the differential role of largely distinct VTA DA neuron populations in response to rewarding vs. aversive stimuli<sup>19</sup>. In addition, our observation that modulation of VTA-NAc but not VTA-mPFC pathway induces anhedonic-like effects suggests a functional role for the VTA-NAc, but not VTA-mPFC, pathway in encoding reward-related information in the context of depression. Our projection specific findings thus provide fundamentally new insights into the complex role played by VTA DA neurons in an individual’s adaptations to repeated stress and the development of depression-like behavioural abnormalities.

## METHODS

### Experimental subjects

CD1 male retired breeders (Charles River), C57BL/6J male mice (7–9 weeks; Jackson Laboratories) and Tyrosine hydroxylase (TH)-Cre male transgenic mice (7–9 weeks; Charles Rivers) were used in these studies. TH-Cre transgenic mice (EM:00254) were obtained from the European Mutant Archive and mated with C57BL/7 wild-type mice<sup>7,31</sup>. All TH-Cre subjects used in this study were backcrossed for at least 10 generations. Mice were singly housed and maintained on a 12-hr light/dark cycle with food and water available *ad libitum*. All animal protocols were in accordance with the National Institutes of Health Guide for Care and Use of Laboratory Animals and approved by the Mount Sinai Institutional Animal Care and Use Committee.

### Virus vectors

AAV-DIO-ChR2-EYFP, AAV-DIO-NpHR-EYFP and AAV-DIO-EYFP virus plasmids<sup>32</sup> were initially generated by previous protocols<sup>33</sup> and more recently purchased from

University of North Carolina vector core facility (UNC). HSV-ChR2-EYFP and HSV-EYFP were provided by Rachael Neve's laboratory (MIT). Retrograde pseudorabies virus (PRV)-Cre was engineered by Jeffrey Friedman's laboratory (Rockefeller University).

### **Stereotaxic surgery, viral mediated gene transfer, cannula placement and optic fiber placement**

Mice were anesthetized with ketamine (100mg/kg)/xylazine (10mg/kg) and their skull was exposed by scalpel incision. For ChR2 viruses, thirty-three gauge needles were placed either bilaterally or unilaterally at a 0° angle into the VTA (AP -3.3; LM +0.5; DV -4.4 in the mm) and 0.5–1µl of virus was infused at a rate of 0.1 µl/min. NpHR virus was injected bilaterally into the VTA at a 7° angle (AP -3.3 mm; LM +1.05 mm; DV -4.6 mm) and 1 µl of virus was infused at a rate of 0.1µl/min. For PRV-Cre viral injections thirty-three gauge needles were placed bilaterally at either a 10° angle into the NAc (AP +1.6mm; LM +1.5mm; DV -4.4mm) or 15° angle into the mPFC (AP +1.7; LM +0.75; DV -2.5) and 0.5–1 µl of virus was infused at a rate of 0.1 µl/min. Bilateral (26 gauge) or unilateral (20 gauge) cannula 3.9 mm length from the cannula base were implanted over the VTA (AP -3.3; LM +0.5; DV -3.7). For secure fixture of the cannula to the skull, instant adhesive (Loctite 454) was placed between the base of the cannula and the skull followed by addition of dental cement (Ortho-Jet) around the cannula and the skull. For NpHR-expressing viral vectors, we used the chronically implantable optical fiber system<sup>34</sup>. Chronically implantable fibers were homemade with 200 µm core optic fiber and were implanted into the VTA at a 7° angle (AP -3.3 mm; LM +1.05 mm; DV -4.4 mm). For secure fixture of the implantable fiber to the skull, the skull was dried followed by addition of industrial strength dental cement (Grip cement; Dentsply) between the base of the implantable fiber and the skull. For AAV surgeries on TH-Cre mice (cell specific study), we performed two surgeries where we first injected the ChR2 virus then performed cannula surgery at least 2 weeks later when the AAV virus was expressed. Mice were allowed to recover for at least 3 days before starting the behavioural paradigm. For AAV surgeries on C57 mice (projection specific study) we again undertook 2 surgeries, where ChR2 virus surgery was performed first followed by PRV-Cre and cannula/implantable fiber surgery at least 2 weeks later. In order to allow the mice to recover and for PRV-Cre to retrograde back to the VTA we waited 5 days before starting the behavioural paradigm. For HSV surgeries both ChR2 virus and cannula placement was performed on the same day and mice were allowed to recover for at least 3 days prior to starting the behavioural paradigm. Lumaflour tracing for retrograde labeling of VTA neurons projecting to NAc or mPFC, the retrobeads were injected into the NAc or mPFC at the coordinates mentioned previously. 1µl of lumaflour was injected into each hemisphere.

For *in vivo* optical control of VTA neuronal firing with ChR2 experiments, a 200 µm core optic fiber was modified for attachment to the cannula. When the fiber was secured to the cannula the tip of the fiber extended about 0.5 mm beyond the cannula. This experimental set up was based on and slightly modified from previous studies<sup>14,35</sup>. For NpHR experiments 200µm fiber core was attached to an chronically implanted fiber. Optic fibers were only secured *in vivo* during the behavioural paradigm (during subthreshold social defeat or social interaction test).

### Blue light stimulation

Optical fibers (Thor Labs, BFL37-200) were connected via a FC/PC adaptor to a 473 nm blue laser diode (Crystal Laser, BCL-473-050-M), and a stimulator (Agilent Technologies, #33220A) was used to generate blue light pulses. For *in vitro* slice electrophysiological validation of ChR2 activation we tested 0.1–50Hz stimulation protocols. For *in vivo* optrode recordings we tested similar stimulation protocols. For all *in vivo* behavioural experiments, mice were given, either, low frequency, tonic (0.5Hz, 15 ms) or high frequency, phasic (20Hz, 40 ms) light stimulations. In both tonic and phasic light stimulation protocols, VTA DA neurons were exposed to 5 spikes over each 10 second period (Fig. 1c). For ChR2 activation during the subthreshold social defeat, mice received bilateral stimulation, while for all ChR2 activation during the social interaction test mice received unilateral stimulations.

### Yellow light stimulation

Optical fibers (Thor Labs, SFS200/220Y) were connected via a FC/PC adaptor to a 561 nm yellow laser diode (Crystal Laser, CL561-050-L), and a stimulator (Agilent Technologies, #33220A) was used to generate yellow light pulses. For *in vitro* slice electrophysiological validation of NpHR activation, we tested different durations of yellow light activation (1–60 sec duration). For all *in vivo* behavioural experiments, mice was given a protocol of 8 sec of yellow light on followed by 2 sec off during the social interaction test. All NpHR experiments were performed using bilateral stimulations.

### Social defeat stress and social interaction

Mice underwent either a subthreshold social defeat stress paradigm or a repeated social defeat stress paradigm<sup>36</sup>. The subthreshold paradigm involved placing the test mice (intruder) into the home cage of a, larger, retired 'resident' breeder mouse (CD1) for 2 min during which time the experimental mouse was physically attacked (defeated) by the CD1 mouse. After 2 min of physical interaction, the experimental mice underwent 10 min of sensory stress. For this, a perforated plexiglass partition was placed in the middle of the CD1 mouse home cage, and the resident CD1 and intruder experimental mouse were physically separated but kept next to each other. After 10 min of sensory stress the experimental mouse was returned to its home cage for 5 min after which time it went through a second round of physical interaction and sensory stress in the home cage of a new CD1 mouse. After 2 bouts of defeats the experimental mouse was returned to its home cage and underwent social interaction test the next day. In a subset of experiments the experimental mice underwent bilateral light stimulation (5min/hemisphere), in order to stimulate VTA DA cells, during the sensory stress period.

For the repeated social defeat paradigm, experimental mice were placed into the home cage of a CD1 mouse for 10 min during which time it was physically defeated by the CD1 mouse. After 10 min of physical interaction CD1 and experimental mouse were maintained in sensory contact for 24 hr using a perforated plexiglass partition dividing the resident home cage in two halves. The experimental mice were exposed to a new CD1 mouse home cage for 10 consecutive days and tested on social interaction on day 11. Both subthreshold and repeated social defeat were carried out between 13:00 and 15:00.



Social avoidance behaviour, towards a novel CD1 mouse, was measured in a two-stage social interaction test. In the first 2.5 min test (target absent), the experimental mouse was allowed to freely explore a square shaped arena (44 × 44 cm) containing a wire mesh cage (10 × 6 cm) placed on one side of the arena. In the second 2.5 min test, the experimental mouse was reintroduced back into the arena with an unfamiliar CD1 mouse contained behind a wire mesh cage. Video tracking software (Ethovision 3.0, Noldus) was used to measure the amount of time the experimental mouse spent in the “Interaction Zone” (14 × 26 cm), “Corner Zone” (10 × 10 cm) and “Total Travel” within the arena. In a subset of studies experimental mice underwent unilateral blue light stimulation in order to activate the VTA DA cells or yellow light stimulation to inhibit VTA DA cells, during both the target absent and target present sessions of the social interaction test. The interaction ratio was measured as (interaction time, target present)/(interaction time, target absent) and normalized to 100. Susceptible and resilient mice were segregated based on the interaction ratio: mice with scores <100 were defined as “susceptible” and those with scores ≥ 100 were defined as “unsusceptible” or resilient. To confirm that the optogenetic activation-induced depression-related avoidance is not a simple fear-memory of a CD1 aggressor, a social interaction test using a C57 mouse as a target was carried out. Mice that had undergone subthreshold social defeat followed by phasic stimulation during the social interaction test similarly avoided the non-aggressive C57 social target to the same degree as observed with a CD1 target (Supplementary Fig. 2). This is consistent with our previous work showing that a C57 social target induced social avoidance in the repeated social defeat paradigm<sup>5</sup>.

### Sucrose preference

Mice were initially habituated to 2-bottle (50ml tubes with stoppers fitted with ball-point sipper tubes) choice filled with drinking water two days prior to the sucrose preference measurements. Upon completion of the social interaction test mice were given access to 2-bottle choice of water or 1% sucrose solution. Bottles containing water and sucrose were weighed at several time points during the day at 15:00, 18:00 and 09:00 for 3 days. The position of the bottles were interchanged (left to right, right to left) after each weight measurements in order to ensure that the mice do not develop a side preference. Sucrose preference was calculated as a percentage [ $100 \times \text{Amount of Sucrose Consumed (in bottle A)} / \text{Total volume consumed (bottles A + B)}$ ]. Robust sucrose preference was evident during the first night of measurement (12 hr) and this was used in all subsequent analysis.

### Elevated plus-maze

Mice were placed in the center of an elevated plus-maze (arms are 33 cm × 5 cm, with 25 cm tall walls on the closed arms) and their behaviour was digitally tracked for 5 min. Mice received VTA optical stimulation during the whole duration of the elevated plus-maze. A video tracking system (Ethovision 3.0, Noldus) was used to measure amount of time spent in the closed and open arms.

### Open Field

Mice were tested for their activity during 15 min in an open field arena (44 × 44 cm). A video tracking system (Ethovision 3.0, Noldus) was used to measure the locomotor activity

of the animal, as well as the time spent in the center (34cm × 34cm) and periphery of the test arena.

### ***In vitro* patch-clamp electrophysiology**

Whole cell optogenetic recordings were obtained from VTA DA neurons in acute brain slices from A) TH-Cre mice that had been stereotaxically injected into the VTA with AAV-DIO-ChR2-EYFP or B) C57 mice that been injected with HSV-ChR2-EYFP into the VTA or C) C57 mice that been injected with the retrograde viral vector PRV-Cre in either the NAc or mPFC and AAV-DIO--ChR2-EYFP or AAV-DIO-NpHR-EYFP into the VTA. Cell attached recordings were obtained from VTA DA neurons in acute brain slices from wild type C57 mice that had been stereotaxically injected with the retrograde dye lumafuor in either NAc or mPFC. To minimize stress and to obtain healthy VTA slices, mice were anesthetized and perfused immediately for 40–60 seconds with ice-cold aCSF (artificial cerebrospinal fluid), which contained 128 mM NaCl, 3 mM KCl, 1.25 mM NaH<sub>2</sub>PO<sub>4</sub>, 10mM D-glucose, 24 mM NaHCO<sub>3</sub>, 2 mM CaCl<sub>2</sub> and 2 mM MgCl<sub>2</sub> (oxygenated with 95% O<sub>2</sub> and 5% CO<sub>2</sub>, pH 7.4, 295–305 mOsm). Acute brain slices containing VTA DA neurons were cut using a microslicer (DTK-1000, Ted Pella) in cold sucrose-aCSF, which was derived by fully replacing NaCl with 254 mM sucrose and saturated by 95% O<sub>2</sub> and 5% CO<sub>2</sub>. Slices were maintained in holding chamber with aCSF for 1 hr at 37°C. Patch pipettes (3–5 mΩ) for whole cell current-clamp, voltage-clamp and cell attached recordings were filled with internal solution containing the following: 115 mM potassium gluconate, 20 mM KCl, 1.5 mM MgCl<sub>2</sub>, 10 mM phosphocreatine, 10 mM HEPES, 2 mM magnesium ATP and 0.5 mM GTP (pH 7.2, 285 mOsm). Whole cell and cell-attached recordings were carried out using aCSF at 34°C (flow rate = 2.5ml/min). For whole cell recordings during optogenetic stimulation resting membrane potential and action potentials were recorded in current clamp mode and inward current measurements were made in voltage clamp mode using the Multiclamp 700B amplifier and data acquisition was done in pClamp 10 (Molecular Devices). Series resistance was monitored during the experiments and membrane currents and voltages were filtered at 3KHz (Bessel filter). For ChR2 experiments, sustained and trains (0.1–50Hz) of blue light were generated by a stimulator mentioned above and delivered to VTA DA neurons expressing ChR2 through a 200 mm optic fiber attached to a 473 nm laser. For NpHR experiments, different durations of yellow light were generated by a stimulator mentioned above and delivered to VTA DA neurons expressing NpHR through a 200 mm optic fiber attached to a 561 nm laser. For cell-attached action potential recordings, signals were band pass filtered at 300Hz-1KHz to identify DA neurons and bessel filtered at 10KHz (gain 50) using a Multiclamp 700B amplifier and data acquisition was done in pClamp 10. For measurements of the spontaneous activity of VTA DA neurons, cell attached recordings were performed. To measure the intrinsic membrane properties of VTA DA neurons, whole cell recordings were carried out in current clamp mode following incremental steps of current injection (step 50 pA; range 50–200 pA).

### ***In vivo* optrode recording**

Viral injection and *in vivo* optrode recordings were carried out as described previously<sup>7,37</sup>. AAV-DIO-ChR2-EYFP was injected into VTA (AP –3.44; LM +0.48; DV –4.4) of TH-Cre mice and left for at least 2 weeks to allow for viral expression. Prior to recordings mice were

deeply anesthetized with a ketamine/xylazine mixture and placed on a stereotactic frame and attached to a temperature regulator. The skull directly above the VTA was removed and an optrode consisting of a tungsten electrode (1m $\Omega$  ~ 125 $\mu$ m) tightly bundled with an optical fiber (200 $\mu$ m core, 0.2 NA) was lowered to the boundary of the VTA (AP -3.44; LM +0.48; DV -4). The tip of the electrode protruded about 0.4mm beyond the optical fiber to ensure illumination of the recorded neurons. At the VTA boundary simultaneous optical stimulation and electrical response of neurons expressing ChR2 was carried out as the optrode was gradually lowered at 0.1mm increments until a good response was measured. The optical fiber was coupled to a 473nm solid state laser diode with a ~20mW output. Recorded signals were band-pass filtered at 300Hz-5KHz using an 1800 Microelectrode AC amplifier.

### Immunohistochemistry

For double-immunofluorescence experiments, tissue sections were fixed in 4% (wt/vol) PBS-buffered paraformaldehyde. Tissues and cells were blocked in PBS-T (0.3% Triton X-100) including 2% (wt/vol) BSA (Sigma) and then exposed overnight to the following primary antibody mixtures: anti-GFP (invitrogen, 1:2000) and anti-TH (sigma, 1:10,000). Detection of primary antibodies was performed with mixtures of the secondary antibodies Cy2-anti-mouse and Cy3-conjugated anti-rabbit (1:500; Jackson ImmunoResearch). Anti-NeuN (Aves Labs, NUN) was raised from chicken was used at a dilution ratio of 1:1000 and was detected by CY3-anti-chicken. For TH labeling, anti-TH (sigma) from mouse at a dilution ratio of 1:5000 was used and is detected by CY5-anti-mouse. For GFP labeling, anti-GFP (invitrogen) from rabbit was used at a dilution ratio of 1:2000 and was detected by CY2-anti-rabbit. Tissues and cells were counterstained and mounted with antifade solution, including DAPI (VectaShield; Vector Laboratories). Sections were subsequently imaged (20x) on a LSM 710 confocal (Zeiss). Cell counting was carried out manually using Image J. For immuno validation of PRV-Cre, animals were killed with a lethal dose of Isoflurane and then transcardially perfused with PBS then 10% formalin 5–10 days post-PRV-Cre injections. Following perfusion, brains were kept in 10% formalin at 4°C for 18–24 hr, at which point the brains were transferred to PBS and sliced into coronal sections using a vibrating blade microtome (Leica Microsystems, model VT1000S). For immunostaining, we processed the slices using antibodies against GFP (Abcam, chicken, 1:1000) and tyrosine hydroxylase (Pel-Freez, rabbit, 1:1000). The antibodies were labeled with goat anti-chicken Alexa 488 and goat anti-rabbit Alexa 633 (Invitrogen, 1:1000), respectively. mCherry expression from the AAV was sufficiently intense for confocal microscopy. Sections were imaged at 20x for analysis, which was performed manually.

### Supplementary Material

Refer to Web version on PubMed Central for supplementary material.

### Acknowledgments

This work was supported by the National Institute of Mental Health (R01 MH092306: D.C., M.H.H.), Johnson & Johnson/IMHRO Rising Star Translational Research Award (M.H.H.), National Research Service Awards (F31 MH095425: J.J.W.; F32 MH096464: A.K.F), and Mount Sinai PREP R25 GM064118 (B.J.). We would like to thank Keya Roy for help in drawing some of the schematics in the figures, and thank Roger Cachepe and Joseph Cheer for help in teaching chronic fiber implantation techniques.

## LITERATURE CITATIONS

1. Willner P, Hale AS, Argyropoulos S. Dopaminergic mechanism of antidepressant action in depressed patients. *J Affect Disord.* 2005; 86:37–45. [PubMed: 15820269]
2. Nestler EJ, Carlezon WA Jr. The mesolimbic dopamine reward circuit in depression. *Biol Psychiatry.* 2006; 59:1151–1159. [PubMed: 16566899]
3. Berton O, Nestler EJ. New approaches to antidepressant drug discovery: beyond monoamines. *Nat Rev Neurosci.* 2006; 7:137–151. [PubMed: 16429123]
4. Yadid G, Friedman A. Dynamics of the dopaminergic system as a key component to the understanding of depression. *Prog Brain Res.* 2008; 172:265–286. [PubMed: 18772037]
5. Krishnan V, et al. Molecular adaptations underlying susceptibility and resistance to social defeat in brain reward regions. *Cell.* 2007; 131:391–404. [PubMed: 17956738]
6. Grace AA, Floresco SB, Goto Y, Lodge DJ. Regulation of firing of dopaminergic neurons and control of goal-directed behaviors. *Trends Neurosci.* 2007; 30:220–227. [PubMed: 17400299]
7. Tsai HC, et al. Phasic firing in dopaminergic neurons is sufficient for behavioral conditioning. *Science.* 2009; 324:1080–1084. [PubMed: 19389999]
8. Cao JL, et al. Mesolimbic dopamine neurons in the brain reward circuit mediate susceptibility to social defeat and antidepressant action. *J Neurosci.* 2010; 30:16453–16458. [PubMed: 21147984]
9. Schultz W. Dopamine signals for reward value and risk: basic and recent data. *Behav Brain Funct.* 2010; 6:24. [PubMed: 20416052]
10. Berton O, et al. Essential role of BDNF in the mesolimbic dopamine pathway in social defeat stress. *Science.* 2006; 311:864–868. [PubMed: 16469931]
11. Anstrom KK, Miczek KA, Budygin EA. Increased phasic dopamine signaling in the mesolimbic pathway during social defeat in rats. *Neuroscience.* 2009; 161:3–12. [PubMed: 19298844]
12. Razzoli M, Andreoli M, Michielin F, Quarta D, Sokal DM. Increased phasic activity of VTA dopamine neurons in mice 3 weeks after repeated social defeat. *Behav Brain Res.* 2011; 218:253–257. [PubMed: 21129410]
13. Krishnan V, Berton O, Nestler E. The use of animal models in psychiatric research and treatment. *Am J Psychiatry.* 2008; 165:1109. [PubMed: 18765492]
14. Lobo MK, et al. Cell type-specific loss of BDNF signaling mimics optogenetic control of cocaine reward. *Science.* 2010; 330:385–390. [PubMed: 20947769]
15. Iniguez SD, et al. Extracellular signal-regulated kinase-2 within the ventral tegmental area regulates responses to stress. *J Neurosci.* 2010; 30:7652–7663. [PubMed: 20519540]
16. Valenti O, Gill KM, Grace AA. Different stressors produce excitation or inhibition of mesolimbic dopamine neuron activity: response alteration by stress pre-exposure. *Eur J Neurosci.* 2012; 35:1312–1321. [PubMed: 22512259]
17. Ungless MA, Magill PJ, Bolam JP. Uniform inhibition of dopamine neurons in the ventral tegmental area by aversive stimuli. *Science.* 2004; 303:2040–2042. [PubMed: 15044807]
18. Venzala E, Garcia-Garcia AL, Elizalde N, Tordera RM. Social vs. environmental stress models of depression from a behavioural and neurochemical approach. *Eur Neuropsychopharmacol.* Jun 27.2012 [Epub ahead of print].
19. Lammel S, Ion DI, Roeper J, Malenka RC. Projection-specific modulation of dopamine neuron synapses by aversive and rewarding stimuli. *Neuron.* 2011; 70:855–862. [PubMed: 21658580]
20. Willner P. The mesolimbic dopamine system as a target for rapid antidepressant action. *Int Clin Psychopharmacol.* 1997; 12 (Suppl 3):S7–14. [PubMed: 9347387]
21. Radulescu AR. Mechanisms explaining transitions between tonic and phasic firing in neuronal populations as predicted by a low dimensional firing rate model. *PLoS One.* 2010; 5
22. Inyushin MU, Arencibia-Albite F, Vazquez-Torres R, Velez-Hernandez ME, Jimenez-Rivera CA. Alpha-2 noradrenergic receptor activation inhibits the hyperpolarization-activated cation current (I<sub>h</sub>) in neurons of the ventral tegmental area. *Neuroscience.* 2010; 167:287–297. [PubMed: 20122999]

23. Friedman, AK., et al. Essential role of ventral tegmental area dopamine neurons in mediating the induction and rapid reversal of depression-like behaviours. Abstract. The 50th Anniversary Meeting of ACNP; 2011.
24. Berman RM, et al. Antidepressant effects of ketamine in depressed patients. *Biol Psychiatry*. 2000; 47:351–354. S0006-3223(99)00230-9 [pii]. [PubMed: 10686270]
25. Li N, et al. mTOR-dependent synapse formation underlies the rapid antidepressant effects of NMDA antagonists. *Science*. 2010; 329:959–964. [PubMed: 20724638]
26. Autry AE, et al. NMDA receptor blockade at rest triggers rapid behavioural antidepressant responses. *Nature*. 2011; 475:91–95. [PubMed: 21677641]
27. Hemmeter UM, Hemmeter-Spernal J, Krieg JC. Sleep deprivation in depression. *Expert Rev Neurother*. 2010; 10:1101–1115.10.1586/ern.10.83 [PubMed: 20586691]
28. Giacobbe P, Mayberg HS, Lozano AM. Treatment resistant depression as a failure of brain homeostatic mechanisms: implications for deep brain stimulation. *Exp Neurol*. 2009; 219:44–52. [PubMed: 19426730]
29. Sartorius A, et al. Remission of major depression under deep brain stimulation of the lateral habenula in a therapy-refractory patient. *Biol Psychiatry*. 2010; 67:e9–e11. [PubMed: 19846068]
30. Li B, et al. Synaptic potentiation onto habenula neurons in the learned helplessness model of depression. *Nature*. 2011; 470:535–539. [PubMed: 21350486]
31. Lindeberg J, et al. Transgenic expression of Cre recombinase from the tyrosine hydroxylase locus. *Genesis*. 2004; 40:67–73.10.1002/gene.20065 [PubMed: 15452869]
32. Cardin JA, et al. Targeted optogenetic stimulation and recording of neurons in vivo using cell-type-specific expression of Channelrhodopsin-2. *Nat Protoc*. 2010; 5:247–254. [PubMed: 20134425]
33. Hommel JD, Sears RM, Georgescu D, Simmons DL, DiLeone RJ. Local gene knockdown in the brain using viral-mediated RNA interference. *Nat Med*. 2003; 9:1539–1544. [PubMed: 14634645]
34. Sparta DR, et al. Construction of implantable optical fibers for long-term optogenetic manipulation of neural circuits. *Nat Protoc*. 2012; 7:12–23. [PubMed: 22157972]
35. Gradinaru V, et al. Targeting and readout strategies for fast optical neural control in vitro and in vivo. *J Neurosci*. 2007; 27:14231–14238. [PubMed: 18160630]
36. Golden SA, Covington HE 3rd, Berton O, Russo SJ. A standardized protocol for repeated social defeat stress in mice. *Nat Protoc*. 2011; 6:1183–1191. [PubMed: 21799487]
37. Stuber GD, et al. Excitatory transmission from the amygdala to nucleus accumbens facilitates reward seeking. *Nature*. 2011; 475:377–380. [PubMed: 21716290]

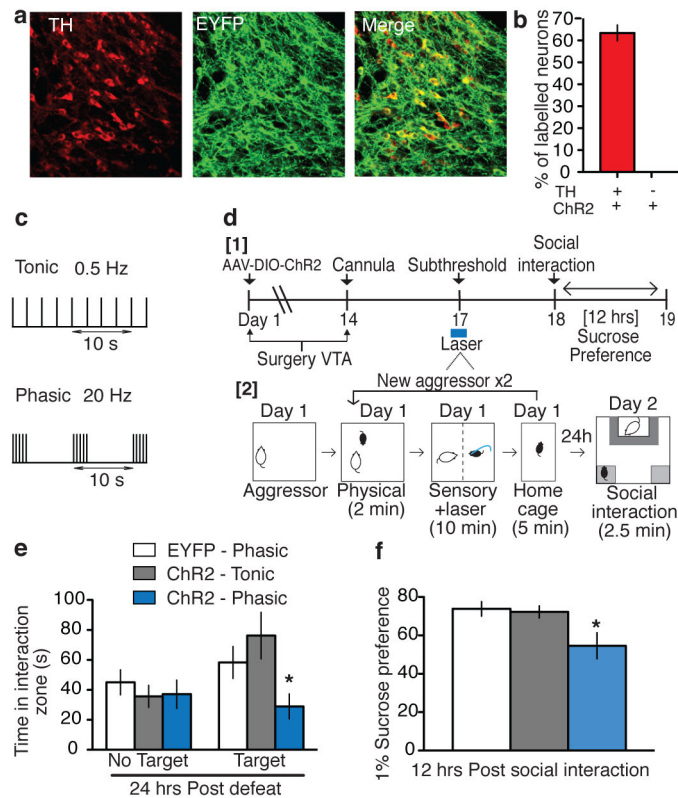


**Figure 1. Phasic, but not tonic, optical stimulation of VTA DA neurons during a subthreshold social defeat induces a susceptible phenotype**

Confocal image showing co-expression of AAV-DIO-ChR2 in TH+ DA cells from TH-Cre mice. **b**, Quantification shows that ChR2-expressing TH+ cells are 62±4% of total TH+ neurons in the VTA and there was no expression of ChR2 in TH- neurons (n=2–3 sections from n=4 animals). **c**, Optical stimulation protocols for mimicking tonic (0.5 Hz) or phasic (20 Hz) firing. Note that for both stimulating protocols, five spikes are induced over each ten second period. **d1**, Experimental timeline. **d2**, Detailed schematic of the subthreshold paradigm showing laser stimulation during social defeat. **e**, Social interaction data in control, tonic, and phasic groups. ( $F_{2,30} = 4.70$ ,  $p < 0.05$ ; *post-hoc* test: \*  $p < 0.05$ ; n=7–14). **f**, Sucrose preference measured over a 12-hr period after the social interaction test ( $F_{2,22} = 5.22$ ,  $p < 0.05$ ; *post-hoc* test, \*  $p < 0.05$ ; n=7–10). All bar graphs depict ± s.e.m.

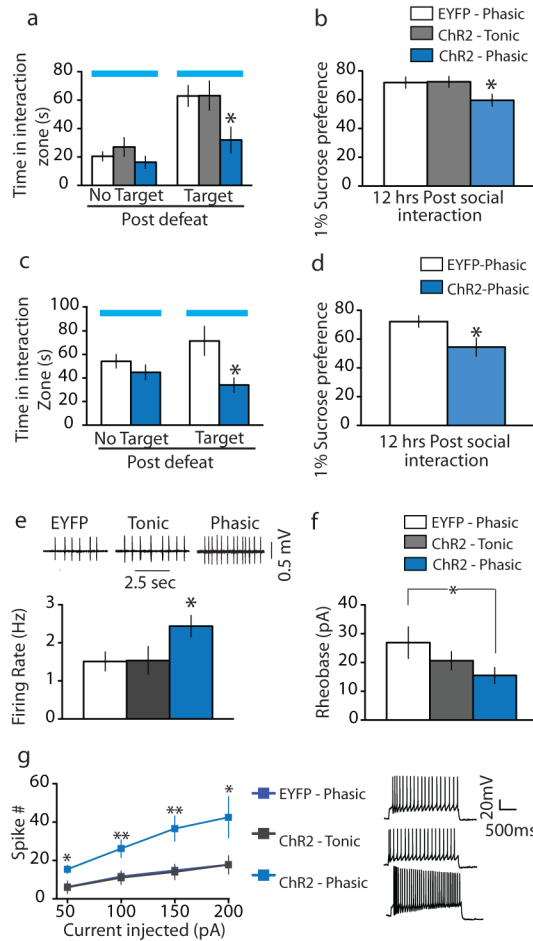


**Figure 2. Phasic optical stimulation of VTA DA neurons during the social interaction test instantly induces a susceptible phenotype in two social defeat paradigms**

**a**, Social interaction data in control, tonic, and phasic groups ( $F_{2,22} = 4.00$ ,  $p < 0.05$ ; *post-hoc* test: \*  $p < 0.05$ ;  $n = 7-11$ ). **b**, Sucrose preference measured over a 12-hr period after the social interaction test ( $F_{2,25} = 3.47$ ,  $p < 0.05$ ; *post-hoc* test: \* denotes  $p < 0.05$ ;  $n = 8-11$ ). **c**, Social interaction data measured on day 17 ( $t_{15} = 2.72$ , \* denotes  $p < 0.05$ ; two tailed  $t$ -test,  $n = 11-18$ ). **d**, Sucrose preference measured over a 12-hr period after the social interaction test ( $t_{17} = 2.34$ , \*  $p < 0.05$ ; two tailed  $t$ -test,  $n = 6-12$ ). **e**, Sample traces: showing *in vitro* spontaneous activity of VTA DA neurons from TH-Cre mice that underwent tonic and phasic stimulation during the social interaction test 24 hr after subthreshold social defeat (see Supplementary Fig. 5j for the experimental timeline). Bar graph: Comparison of spontaneous firing in VTA DA neurons from EYFP-control, tonic, and phasic-stimulated mice ( $F_{2,50} = 3.19$ ,  $p < 0.05$ ; *post-hoc* test, \*  $p < 0.05$ ;  $n = 17-19$ ). **f**, Significantly less current was required to evoke a single spike in phasic stimulated mice compared to EYFP control mice ( $t_{21} = 1.8$ , \*  $p < 0.05$ ; one tailed  $t$ -test,  $n = 12-16$ ). **g**, VTA DA cells from phasic stimulated mice display overall increased cell excitability to incremental steps in current injections (50, 100, 150 and 200pA) compared with EYFP control and tonic stimulated mice ( $F_{2,140} = 16.13$ ,  $p < 0.001$ ; *post-hoc* test, \*  $p < 0.05$  \*\*  $p < 0.005$ ;  $n = 5-17$ ). All bar graphs depict  $\pm$  s.e.m.

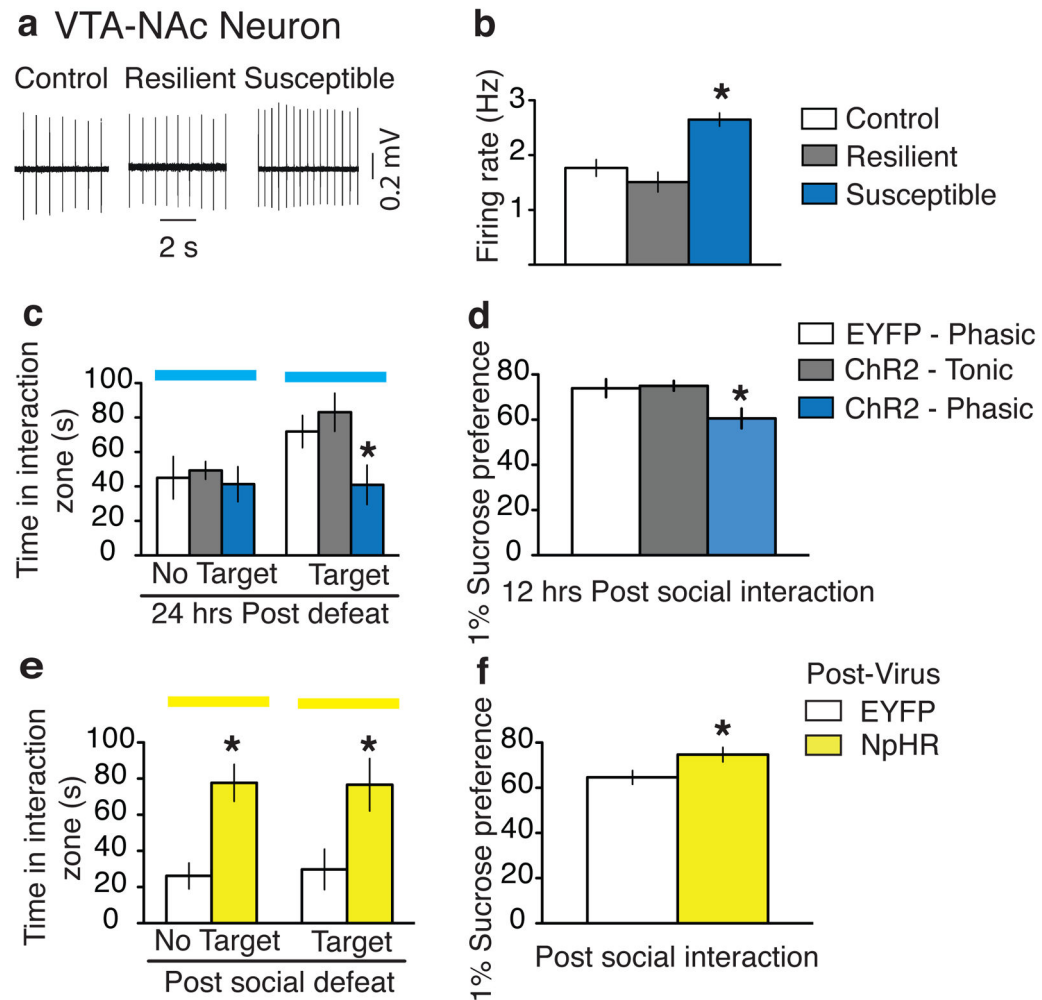


**Figure 3. Bidirectional effect of modulating the VTA-NAc pathway on susceptibility to social defeat**

**a**, Sample traces recorded from VTA-NAc neurons in VTA slices. **b**, Firing rates of VTA-NAc neurons from control, resilient, and susceptible mice ( $F_{2,89} = 15.77$ ,  $p < 0.001$ ; *post-hoc* test, \*  $p < 0.001$ ;  $n = 12-52$ ). **c**, Social interaction data obtained during optical stimulation of VTA-NAc neurons in control, tonic, and phasic groups. ( $F_{2,20} = 4.43$ ,  $p < 0.05$ ; *post-hoc* test: \*  $p < 0.05$ ;  $n = 5-10$ ). **d**, Sucrose preference data measured over a 12-hr period after the social interaction test. ( $F_{2,18} = 4.80$ ,  $p < 0.05$ ; *post-hoc* test, \*  $p < 0.05$ ;  $n = 5-9$ ). **e**, Social interaction during optical inhibition of VTA-NAc neurons in previously susceptible mice (No target:  $t_{15} = 4.2$ , \*  $p < 0.001$ ; two tailed t-test,  $n = 8-9$ ; Target:  $t_{15} = 2.6$ , \*  $p < 0.05$ ; two tailed t-test,  $n = 8-9$ ). **f**, Sucrose preference measured over a 12-hr period after the social interaction test ( $t_{14} = 2.3$ , \*  $p < 0.05$ ; two tailed t-test,  $n = 8-9$ ). All bar graphs depict  $\pm$  s.e.m.



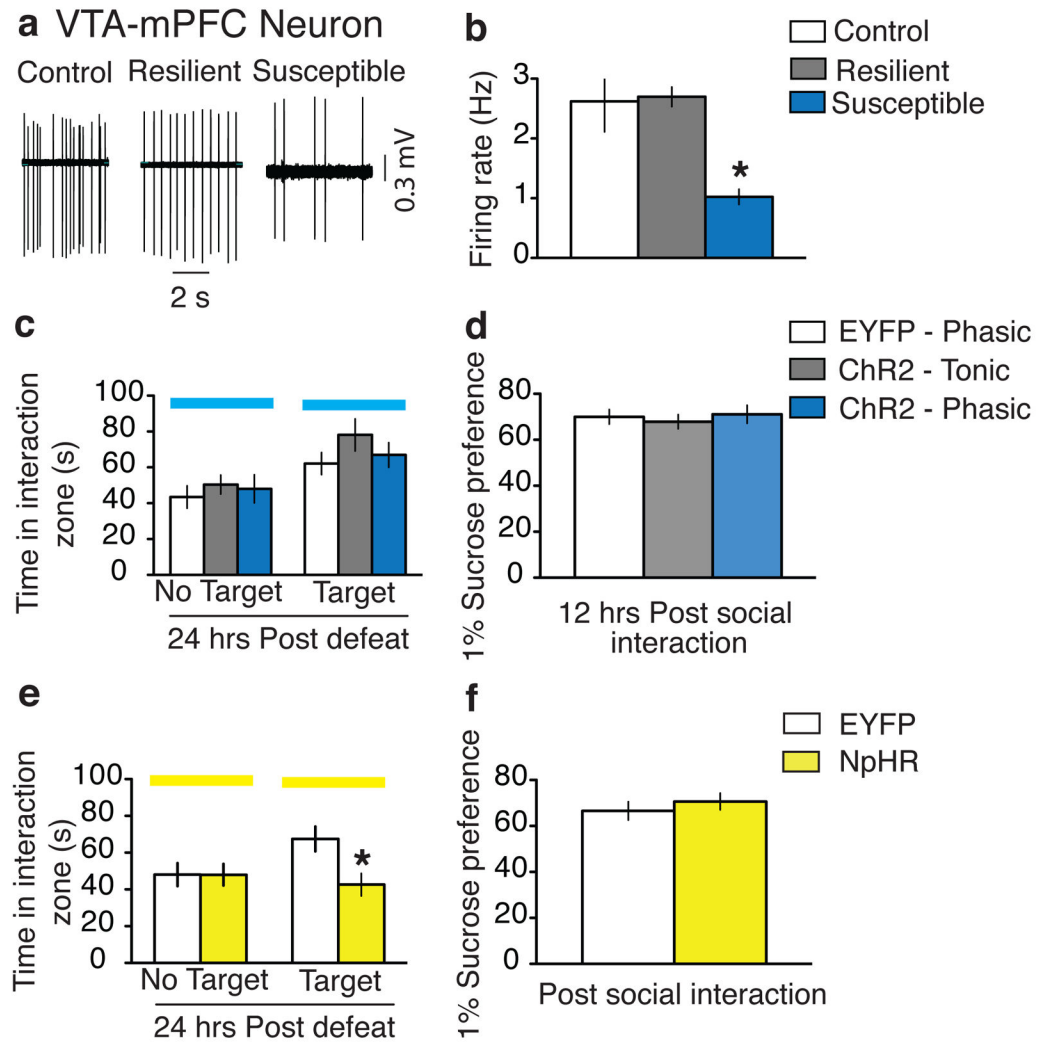


**Figure 4. Effect of modulating the VTA-mPFC pathway on susceptibility to social defeat**  
**a**, Sample traces recorded from VTA-mPFC neurons in VTA slices. **b**, Firing rates of VTA-mPFC neurons from control, resilient, and susceptible mice ( $F_{2,38} = 15.07$ ,  $p=0.0005$ ; *post-hoc* test, \*  $p<0.005$ ;  $n=11-15$ ). **c**, Social interaction data obtained by optical stimulation of VTA-mPFC neurons in control, tonic, and phasic groups ( $F_{2,39} = 1.29$ ,  $p=0.29$ ;  $n=11-17$ ). **d**, Sucrose preference data measured over a 12-hr period after the social interaction test ( $F_{2,33} = 0.19$ ,  $p=0.82$ ;  $n=10-16$ ). **e**, Social interaction data obtained during optical inhibition of VTA-mPFC neurons ( $t_{29} = 2.5$ , \*  $p<0.05$ ; two tailed t-test,  $n=12-19$ ). **f**, Sucrose preference measured over a 12-hr period after the social interaction test ( $t_{29}=0.38$ ,  $p>0.05$ ,  $n=12-19$ ). All bar graphs depict  $\pm$  s.e.m.